Quantum Phases of Quadrupolar Fermi Gases in Optical Lattices

S. G. Bhongale,[1] L. Mathey,[2] Erhai Zhao,[1] S. F. Yelin,[3,4,5] and Mikhail Lemeshko[4,5,*]

[1]*School of Physics, Astronomy, and Computational Sciences, George Mason University, Fairfax, Virginia 22030, USA*
[2]*Zentrum für Optische Quantentechnologien and Institut für Laserphysik, Universität Hamburg, 22761 Hamburg, Germany*
[3]*Department of Physics, University of Connecticut, Storrs, Connecticut 06269, USA*
[4]*ITAMP, Harvard-Smithsonian Center for Astrophysics, 60 Garden Street, Cambridge, Massachusetts 02138, USA*
[5]*Department of Physics, Harvard University, 17 Oxford Street, Cambridge, Massachusetts 02138, USA*

(Received 20 November 2012; published 8 April 2013)

We introduce a new platform for quantum simulation of many-body systems based on nonspherical atoms or molecules with zero dipole moments but possessing a significant value of electric quadrupole moments. We consider a quadrupolar Fermi gas trapped in a 2D square optical lattice, and show that the peculiar symmetry and broad tunability of the quadrupole-quadrupole interaction results in a rich phase diagram encompassing unconventional BCS and charge density wave phases, and opens up a perspective to create a topological superfluid. Quadrupolar species, such as metastable alkaline-earth atoms and homonuclear molecules, are stable against chemical reactions and collapse and are readily available in experiment at high densities.

DOI: 10.1103/PhysRevLett.110.155301 PACS numbers: 67.85.−d, 71.10.Fd, 75.30.Fv

Quantum gases of ultracold atoms have provided a fresh perspective on strongly correlated many-body states by establishing a highly tunable environment in which both open questions of solid state physics and novel, previously unobserved, many-body states can be studied [1]. An important landmark was reached by cooling and trapping dipolar atoms and molecules, bosonic and fermionic [2–7], near or into quantum degeneracy, which extended the range of features available to quantum simulation in ultracold atom systems beyond contact interactions. Numerous exotic states such as supersolids, quantum liquid crystals, and bond-order solids have been predicted; extended Hubbard models with 3-body interactions, and highly tunable lattice spin models for quantum magnetism have been proposed [8–13]. The crucial feature of the interactions in dipolar gases is their anisotropic and long-range character tunable with static and radiative fields [13–15], which is key to the intriguing many-body effects that have been predicted.

In this Letter, we propose to study quadrupolar quantum gases. This constitutes a new class of systems in ultracold physics, which can be used as a platform for quantum simulation. Quadrupole interactions are most visible for nonpolar particles which possess a significant electric quadrupole moment. The angular dependence of the resulting quadrupole-quadrupole interaction is substantially different compared to the dipole-dipole one, due to the higher-order symmetry. For atoms or molecules in an optical lattice, this allows for broad tunability of the nearest- and next-nearest-neighbor couplings. As a concrete example, we discuss metastable alkaline-earth atoms and homonuclear molecules which have comparatively large quadrupolar moments. In order to demonstrate rich many-body effects that arise in ensembles of such particles, we derive the quantum phase diagram of a quadrupolar fermionic gas in an optical lattice at half-filling. We find that several unconventional phases emerge, such as bond order solids and p-wave pairing, and discover the intriguing possibility of creating topological ground states of $p_x + ip_y$ symmetry. While dipolar quantum gases were also shown to host novel many-body phases, quadrupolar particles are available in experiment at higher densities and are stable against chemical reactions [16] and collapse [17].

In order to determine the quadrupole-quadrupole interaction energy, we consider the potential of a classical quadrupole with moment $q = \int \rho(\vec{r}) r^2 (3\cos^2\theta - 1) d\vec{r}$ located at $\vec{r}_0 = 0$ aligned in $\hat{k}$ direction. Here $\rho(\vec{r})$ is the electron charge density and $\cos\theta \equiv \hat{k}\cdot\hat{r}$ [18]. In this Letter, we focus on systems possessing cylindrical symmetry, for which only one component q of the quadrupole moment tensor q_{ij} is nonzero. The electric field potential generated by the quadrupole is given by $\phi(\vec{r}) = \frac{q}{4r^3}(3\cos^2\theta - 1)$. If a second quadrupole with the same alignment $\hat{k}$ is placed at location $\vec{r}$, the resulting interaction energy is $V_{cl}^{qq} = \frac{q}{4}(\hat{k}\cdot\nabla)(\hat{k}\cdot\nabla\phi) = \frac{3q^2}{16r^5}(35\cos^4\theta - 30\cos^2\theta + 3)$. While the functional form of this potential carries over to the quantum description, the prefactor of the interaction for two states has to be obtained via a quantum definition of the quadrupole moment $\mathbf{q}_2$. The latter is a spherical tensor of rank two with components defined in atomic units as $q_{2,M} = -\sum_k r_k^2 C_{2,M}(\theta_k, \phi_k)$, where (r_k, θ_k, ϕ_k) give the coordinates of the kth electron of the particle, and $C_{2,M}(\theta_k, \phi_k) = \sqrt{4\pi/5}\, Y_{2,M}(\theta_k, \phi_k)$ are the reduced spherical harmonics [19]. In the angular momentum basis, $|J, M\rangle$, with M being the projection of the angular momentum, $\mathbf{J}$, onto the quantization axis, the quadrupole operator couples the states with $\Delta J = 0, \pm 2$, so to first order any state with $J > 1/2$ possesses a nonzero quadrupole moment [20]. Thus, the value of the quadrupole moment can be controlled by preparing the particles in a particular $|J, M\rangle$ state, or their combination, using optical or microwave fields. The quadrupole interaction reads

$$V^{qq} = \frac{\sqrt{70}}{r^5} \sum_{\alpha=-2}^{2} (-1)^{\alpha} C_{2,-\alpha}(\theta, \phi)[\mathbf{q}_2^{(1)} \otimes \mathbf{q}_2^{(2)}]_{4,\alpha}, \quad (1)$$

where (r, θ, ϕ) gives the vector between particles, and $[\mathbf{q}_2^{(1)} \otimes \mathbf{q}_2^{(2)}]_{4,\alpha}$ is a spherical tensor of rank four formed from two quadrupole moments. For both particles prepared in the same $|J, M\rangle$ state, Eq. (1) reduces to $V^{qq} = V(3 - 30\cos^2\theta + 35\cos^4\theta)/r^5$, with $V = q^2 3(J^2 + J - 3M^2)^2/[4(4J^2 + 4J - 3)^2]$, where $q = 2\langle 2, 2|q_{2,0}|2, 2\rangle$, which coincides with the classical definition [21]. We note that in the classical limit of $J \to \infty$, and for $M = J$, the prefactor $V = 3q^2/16$ of the classical expression is recovered. The interaction can then be attractive or repulsive depending on the angle θ.

Among the particles for which the quadrupolar moment is known, the most promising candidates for the experimental realization of quadrupolar quantum gases are metastable alkaline-earth atoms [21–25] and homonuclear diatomic molecules [26,27]. Alkaline-earth atoms, such as Sr, and some of the rare-earth atoms, such as Yb, can be prepared in metastable $^3P_2^o$ states, whose lifetime exceeds thousands of seconds [21–25,28], by optical excitation, cf. Fig. 1(a). Both bosonic and fermionic isotopes of Sr and Yb have been brought to quantum degeneracy [29–32]. Ultracold homonuclear molecules, such as Cs_2 or Sr_2, can be prepared in the absolute ground state, $^1\Sigma_g^+(v = 0, J = 0)$, and then transferred to a rotational state with $J > 0$, using a Raman transition [26,27,33], cf. Fig. 1(b). While homonuclear molecules are always bosons, fermionic quadrupolar molecules can be prepared using distinct isotopes of the same species [34]. For both atoms and molecules, the degeneracy of a particular J level can be lifted by an external electric or magnetic field, $\mathbf{F}$. We consider the regime when the quadrupole-quadrupole interactions dominate the behavior of the system; i.e., the electric field $\mathbf{F}$ is too weak to induce a substantial value of a dipole moment, or the particles are prepared in a nonmagnetic Zeeman component. The typical "shapes" of quadrupolar states are exemplified in Fig. 1(c). Both atoms and molecules can be prepared in the $|2, 0\rangle$ ($|2, 2\rangle$) states using two linearly (circularly) polarized photons; the quadrupole-quadrupole interaction is equal in these cases and is larger than for the $|2, 1\rangle$ states.

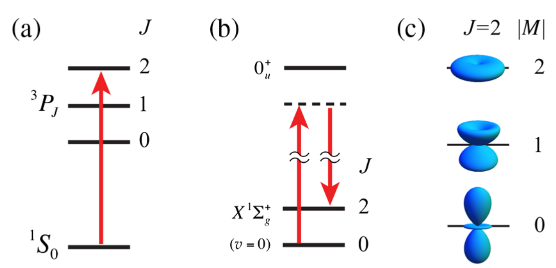

FIG. 1 (color online). Recipe for realization of quadrupolar particles: (a) with alkaline-earth atoms in long-living $^3P_2$ levels; and (b) with homonuclear molecules in rotational states with $J > 1/2$. (c) Angular "shape" of quadrupolar particles exemplified by $|2, M\rangle$ states.

The quadrupole moments for metastable alkaline-earth atoms and homonuclear molecules are similarly on the order of 10–40 a.u. [21–25,27], which gives an interaction strength, V^{qq}, on the order of a few Hz at 266 nm lattice spacing. Furthermore, interactions on the order of 1 kHz can be achieved for 100 nm lattice spacings realizable with atoms trapped in nanoplasmonic structures [35]. We note that the dispersion (van der Waals) interaction, $V^{\mathrm{dis}} \sim r^{-6}$, is 10^2–10^3 times smaller at typical optical lattice spacings [23]; therefore, the quadrupole-quadrupole interaction dominates the physics of these systems. Quantum gases can be trapped for tens of seconds, so the observation of many-body phases generated by these interactions is feasible via the standard techniques, ranging from time-of-flight detection to noise correlation and Bragg spectroscopy.

To illustrate the intriguing many-body effects that can arise in these systems, we investigate the quantum phase diagram of a system of interacting quadrupolar fermions on a square lattice, at half-filling. We assume every particle to be prepared in state $|J, M\rangle$, where $\mathbf{J}$ is the electronic (for atoms) or rotational (for molecules) angular momentum, and M is the projection of $\mathbf{J}$ on the direction $\hat{F} = (\theta_F, \phi_F)$ in the laboratory frame given by the external field $\mathbf{F}$ used to lift the M degeneracy. The particles are confined to a lattice with a lattice constant a_L, corresponding to the Hamiltonian:

$$H = -t\sum_{\langle i,j\rangle} c_i^\dagger c_j + \frac{1}{2}\sum_{i\neq j} V_{ij} c_i^\dagger c_i c_j^\dagger c_j, \quad (2)$$

where t represents the nearest-neighbor hopping and c_i is the fermion annihilation operator at the ith lattice site. Throughout the remainder of the Letter, we use a_L as a unit of length and t as a unit of energy. As schematically shown in Fig. 2(a), the interaction strength V_{ij} depends on the orientation of the vector connecting the quadrupoles, $\mathbf{r} = \mathbf{r}_i - \mathbf{r}_j$, relative to the field direction, $\hat{F}$, via $V_{\mathbf{r}} \equiv V_{ij} = \langle ij|V^{qq}|ij\rangle = V[3 - 30(\hat{r}\cdot\hat{F})^2 + 35(\hat{r}\cdot\hat{F})^4]/r^5$. Thus, one can immediately observe that the interaction between two quadrupoles can be tuned to be either attractive or repulsive, by changing the orientation of the external field $\mathbf{F}$. Fig. 2(b) shows the (θ_F, ϕ_F) dependence of the interaction matrix element between the nearest and next-nearest neighbors. The richness of the quadrupolar interaction becomes apparent in this figure. There are several regions in which the signs and the relative magnitudes of

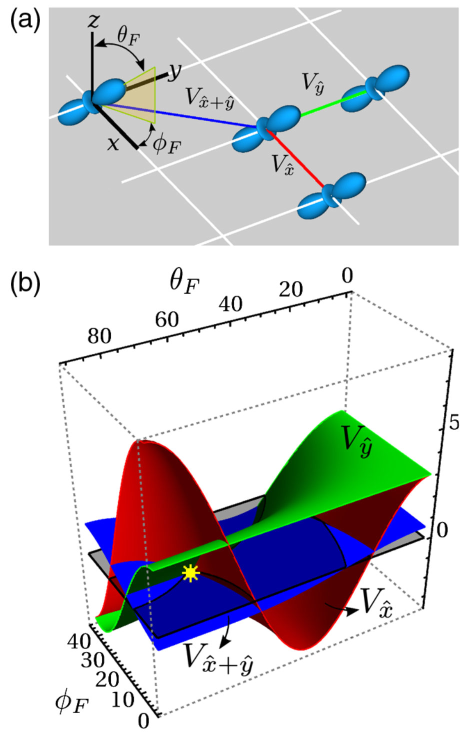

FIG. 2 (color online). (a) Schematic representation of quadrupolar fermions on a square lattice. Alignment of the quadrupoles is given by the quantization axis of the external field **F**, pointing along $\hat{F} = (\theta_F, \phi_F)$. The nearest-neighbor interaction is represented by green and red solid lines, while the next-nearest-neighbor interaction is shown in blue. (b) 3D plot showing the interactions $V_{\hat{x}}$ (red), $V_{\hat{y}}$ (green), and $V_{\hat{x}+\hat{y}}$ (blue) as a function of the angles (θ_F, ϕ_F); "*" marks the point in the vicinity of which both $V_{\hat{x},\hat{y}}$ and $V_{\hat{x}+\hat{y}}$ change the sign.

$\{V_{\hat{x}}, V_{\hat{y}}, V_{\hat{x}+\hat{y}}\}$ show distinctive characteristics. For example, in the region $(\theta_F \lesssim 25°,\ 0° \leq \phi_F \leq 45°)$, both nearest- and next-nearest-neighbor interactions are repulsive, while they all become attractive in the region $(30° \lesssim \theta_F \lesssim 60°, \phi_F \sim 45°)$. Furthermore, one can identify finite regions where either one or two of $\{V_{\hat{x}}, V_{\hat{y}}, V_{\hat{x}+\hat{y}}\}$ is attractive while the rest are repulsive.

Interactions of opposite sign can result in competition between quantum phases of different symmetry, resulting in frustration. Thus, fermions with dominant quadrupolar interactions provide an interesting setup for studying many-body physics with competing phases. For example, in the vicinity of $(90°, 45°)$ both $V_{\hat{x}}$ and $V_{\hat{y}}$ are attractive, while $V_{\hat{x}+\hat{y}}$ is repulsive (see Fig. 2). On general grounds, one would expect a BCS type ground state resulting from condensation of Cooper pairs due to the attractive $V_{\hat{x}}$ and $V_{\hat{y}}$ couplings. However, the repulsive $V_{\hat{x}+\hat{y}}$ interaction, if significant, may lead to the insurgence of some other phase, and therefore, needs to be quantitatively accounted for. As another intriguing example, in the vicinity of $(40°, 5°)$, $V_{\hat{x}}$ is strongly attractive while $V_{\hat{y}}$ is strongly repulsive. As we show below, the ground state in this region is neither a BCS state nor conventional charge density wave (CDW). These two examples show that the actual ground state may be of an unexpected nature. Exposing the true ground state thus demands a theory that is (i) unbiased with respect to the initial ansatz, and (ii) includes fluctuations.

Issue (ii) can be adequately addressed within the renormalization group analysis at weak couplings, where the low energy physics near the Fermi surface is extracted by successively integrating out the high energy degrees of freedom [36]. In order to satisfy criterion (i), we employ the exact (or "functional") renormalization group (FRG) which keeps track of all the interaction vertices, including both the particle-particle and particle-hole channels, and treats all instabilities on equal footing [37,38].

The FRG phase diagram, Fig. 3(a), features several different kinds of BCS and CDW phases with symmetry indicated by the polar plots of Fig. 3(b). CDW_s is a CDW phase with a checkerboard modulation of on-site densities, occurring in regions where the repulsive interaction between nearest neighbors dominates, see Fig. 2. This happens for all values of ϕ_F when $\theta_F \lesssim 25°$, and also for $\phi_F \lesssim 22°$ at large $\theta_F \gtrsim 60°$. In addition, two novel types, CDW_{p_x} and CDW_{p_y}, are present. They correspond to a checkerboard modulation of the effective hopping between nearest neighbors along the x and y direction respectively, i.e., $\langle c_i^\dagger c_j \rangle$ with $\mathbf{r}_i - \mathbf{r}_j = \hat{x}$ or $\hat{y}$, with the average taken over the many-body ground state. We refer to these phases as to bond order solid (BOS) phases. In comparison, the s-wave CDW order corresponds to modulations of $\langle c_i^+ c_i \rangle$. Furthermore, we find a small region of CDW_{s+d} that involves a mixture of extended s and d waves. Together they give rise to a checkerboard modulation of effective hopping between the next-nearest-neighbor sites. The CDW_{p_x}, CDW_{p_y}, and CDW_{s+d} can be thought of as a 2D generalization of the bond-order-wave phase occurring in the extended Hubbard model in one dimension [39–41]. While a BOS is expected for dipolar fermions in 2D [12], it occupies a significantly larger region of the parameter space for quadrupolar interactions (e.g., it is stabilized as soon as θ_F approaches 25°). Moreover, the angular dependence of quadrupolar interactions is substantially more complex, resulting in two BOS phases of p_y and p_x symmetries, appearing at small and large θ_F, respectively. Interestingly, these two phases occur in the regions where $V_{\hat{x}}$ and $V_{\hat{y}}$ are comparable in magnitude but opposite in sign; i.e., $\mathrm{CDW}_{p_x(p_y)}$ is stabilized when $V_{\hat{x}(\hat{y})}$ is repulsive while $V_{\hat{y}(\hat{x})}$ is attractive, cf. Fig. 2(b). Thus, quadrupolar Fermi gases are well suited for exploring the properties of nonzero angular momentum (i.e., unconventional) density wave phases.

Finally, there are two BCS phases, which mostly occur where both $V_{\hat{x}}$ and $V_{\hat{y}}$ are attractive. Our FRG analysis shows that the BCS phase can be stable even though the next-nearest-neighbor interaction is weakly repulsive.

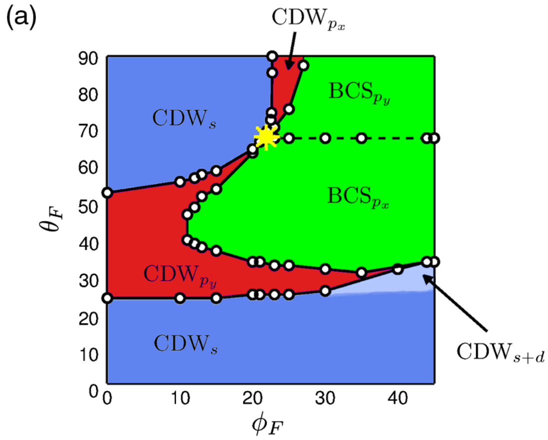

FIG. 3 (color online). Quantum phase diagram for quadrupolar fermions on a square lattice. (a) FRG phase diagram in the weak coupling limit, $V/t = 0.2$, and at half filling shown as a function of the magnetic field direction $\hat{F} = (\theta_F, \phi_F)$. The point marked by "*", where 5 different phases seem to meet, corresponds to $V_{\hat{x}}, V_{\hat{y}}, V_{\hat{x}+\hat{y}} \approx 0$ as shown in Fig. 2(b). This suggests the likelihood of at most three distinct tricritical points in close proximity to each other, which are hard to resolve due to the smallness of the couplings. (b) The orbital symmetry of the CDW and BCS phases shown in (a) is plotted in red. This symmetry corresponds to the symmetry of the most divergent eigenvector of the BCS and CDW vertices combined. The p_x (p_y) wave CDW has the same orbital structure as the p_x (p_y) wave BCS.

We find that the symmetry of the BCS order parameter is p_x or p_y, depending on whether $V_{\hat{x}}$ or $V_{\hat{y}}$ is more attractive. Along the line of $\theta_F \sim 65°$, these two BCS phases are degenerate. This raises the possibility of realizing $p_x + ip_y$ topological superfluid order. By analogy with the proposal of Ref. [42], using an ac field to periodically modulate the direction of (θ_F, ϕ_F), one can lift the degeneracy and engineer the chiral $p_x + ip_y$ state.

In conclusion, we have shown that ultracold Fermi gases with quadrupole-quadrupole interactions can be used to study unconventional BCS, CDW, and topological phases, and gain insight into the physics of competing ground states. While we have focused on the specific case of a square lattice at half-filling, the functional renormalization group methods of this Letter can be applied to study other fillings and lattice geometries. Temperatures achieved for degenerate Fermi gases of alkaline-earth atoms in experiment are $T = 0.26T_F$ and $T = 0.37T_F$ respectively [31,32]. The optimal T_c for the CDW and BCS phases predicted here is estimated to be on the order of $0.03T_F$, for intermediate couplings, $V \sim t$. Thus, these many-body phases seem to be within experimental reach in the near future.

Since quadrupolar interactions occur in numerous subfields of physics, from molecular photofragmentation [43] and structure of f electron compounds [44] to nuclear reactions [45] and gravitation of black holes [46], the proposed quantum simulation platform can in principle be applied beyond the many-body physics of fermionic gases. Finally, we note that ground-state atoms can be provided with significant quadrupole moments by means of Rydberg dressing, i.e., admixing a highly excited electronic state possessing a large quadrupole moment with far-detuned laser light [47,48].

We are grateful to Charles Clark, Robin Coté, Hendrik Weimer, and Shan-Wen Tsai for discussions. S. G. B. and E. Z. are supported by NSF (Grant No. PHY-1205504) and NIST (Grant No. 60NANB12D244). L. M. acknowledges support from the Landesexzellenzinitiative Hamburg, which is financed by the Science and Research Foundation Hamburg and supported by the Joachim Herz Stiftung, and from the Deutsche Forschungsgemeinschaft under Grant No. SFB 925. M. L. acknowledges support from NSF through a grant for the Institute for Theoretical Atomic, Molecular, and Optical Physics at Harvard University and Smithsonian Astrophysical Observatory. S. F. Y. acknowledges financial support from the National Science Foundation and Air Force Office of Scientific Research.

*mlemeshko@cfa.harvard.edu

[1] I. Bloch, J. Dalibard, and W. Zwerger, Rev. Mod. Phys. **80**, 885 (2008).
[2] K. K. Ni, S. Ospelkaus, M. H. G. de Miranda, A. Pe'er, B. Neyenhuis, J. J. Zirbel, S. Kotochigova, P. S. Julienne, D. S. Jin, and J. Ye, Science **322**, 231 (2008).
[3] A. Chotia, B. Neyenhuis, S. A. Moses, B. Yan, J. P. Covey, M. Foss-Feig, A. M. Rey, D. S. Jin, and J. Ye, Phys. Rev. Lett. **108**, 080405 (2012).
[4] J. Deiglmayr, A. Grochola, M. Repp, K. Mörtlbauer, C. Glück, J. Lange, O. Dulieu, R. Wester, and M. Weidemüller, Phys. Rev. Lett. **101**, 133004 (2008).
[5] A. Griesmaier, J. Werner, S. Hensler, J. Stuhler, and T. Pfau, Phys. Rev. Lett. **94**, 160401 (2005).
[6] M. Lu, N. Q. Burdick, and B. L. Lev, Phys. Rev. Lett. **108**, 215301 (2012).

[7] K. Aikawa, A. Frisch, M. Mark, S. Baier, A. Rietzler, R. Grimm, and F. Ferlaino, Phys. Rev. Lett. **108**, 210401 (2012).
[8] M. A. Baranov, Phys. Rep. **464**, 71 (2008).
[9] T. Lahaye, C. Menotti, L. Santos, M. Lewenstein, and T. Pfau, Rep. Prog. Phys. **72**, 126401 (2009).
[10] B. Capogrosso-Sansone, C. Trefzger, M. Lewenstein, P. Zoller, and G. Pupillo, Phys. Rev. Lett. **104**, 125301 (2010).
[11] B. M. Fregoso and E. Fradkin, Phys. Rev. Lett. **103**, 205301 (2009).
[12] S. G. Bhongale, L. Mathey, S. W. Tsai, C. W. Clark, and E. Zhao, Phys. Rev. Lett. **108**, 145301 (2012).
[13] A. V. Gorshkov, S. R. Manmana, G. Chen, E. Demler, M. D. Lukin, and A. M. Rey, Phys. Rev. A **84**, 033619 (2011).
[14] M. Lemeshko, Phys. Rev. A **83**, 051402(R) (2011).
[15] M. Lemeshko, R. V. Krems, and H. Weimer, Phys. Rev. Lett. **109**, 035301 (2012).
[16] S. Ospelkaus, K.-K. Ni, D. Wang, M. H. G. de Miranda, B. Neyenhuis, G. Quéméner, P. S. Julienne, J. L. Bohn, D. S. Jin, and J. Ye, Science **327**, 853 (2010).
[17] T. Koch, T. Lahaye, J. Metz, B. Fröhlich, A. Griesmaier, and T. Pfau, Nat. Phys. **4**, 218 (2008).
[18] In contrast to a dipole, which is analogous to a single-headed arrow (↑) pointing in a particular direction, a quadrupole corresponds to a double-headed arrow (↕) not favoring one direction over another, and, therefore, it can be aligned, but not oriented.
[19] D. A. Varshalovich, A. N. Moskalev, and V. K. Khersonski, *Quantum Theory of Angular Momentum* (World Scientific, Singapore, 1988).
[20] Note the difference with dipole moments which can be nonzero only for states of indefinite parity (superposition of odd and even J's).
[21] A. Derevianko, Phys. Rev. Lett. **87**, 023002 (2001).
[22] B. B. Jensen, H. Ming, P. G. Westergaard, K. Gunnarsson, M. H. Madsen, A. Brusch, J. Hald, and J. W. Thomsen, Phys. Rev. Lett. **107**, 113001 (2011).
[23] R. Santra, K. V. Christ, and C. Greene, Phys. Rev. A **69**, 042510 (2004).
[24] R. Santra and C. H. Greene, Phys. Rev. A **67**, 062713 (2003).
[25] A. A. Buchachenko, Eur. Phys. J. D **61**, 291 (2011).
[26] R. V. Krems, W. C. Stwalley, and B. Friedrich, *Cold Molecules: Theory, Experiment, Applications* (Taylor & Francis, London, 2009).
[27] J. N. Byrd, R. Côté, and J. A. Montgomery, J. Chem. Phys. **135**, 244307 (2011).
[28] S. B. Nagel, C. E. Simien, S. Laha, P. Gupta, V. S. Ashoka, and T. C. Killian, Phys. Rev. A **67**, 011401(R) (2003).
[29] T. Fukuhara, S. Sugawa, and Y. Takahashi, Phys. Rev. A **76**, 051604 (2007).
[30] S. Stellmer, M. K. Tey, B. Huang, R. Grimm, and F. Schreck, Phys. Rev. Lett. **103**, 200401 (2009).
[31] B. J. DeSalvo, M. Yan, P. G. Mickelson, Y. N. M. de Escobar, and T. C. Killian, Phys. Rev. Lett. **105**, 030402 (2010).
[32] T. Fukuhara, Y. Takasu, M. Kumakura, and Y. Takahashi, Phys. Rev. Lett. **98**, 030401 (2007).
[33] I. Manai, R. Horchani, H. Lignier, P. Pillet, D. Comparat, A. Fioretti, and M. Allegrini, Phys. Rev. Lett. **109**, 183001 (2012).
[34] S. B. Papp and C. E. Wieman, Phys. Rev. Lett. **97**, 180404 (2006).
[35] M. Gullans, T. Tiecke, D. E. Chang, J. Feist, J. D. Thompson, J. I. Cirac, P. Zoller, and M. D. Lukin, Phys. Rev. Lett. **109**, 235309 (2012).
[36] R. Shankar, Rev. Mod. Phys. **66**, 129 (1994).
[37] D. Zanchi and H. J. Schulz, Phys. Rev. B **61**, 13 609 (2000).
[38] See Supplemental Material at http://link.aps.org/supplemental/10.1103/PhysRevLett.110.155301 for details on the FRG approach.
[39] M. Nakamura, Phys. Rev. B **61**, 16 377 (2000).
[40] P. Sengupta, A. W. Sandvik, and D. K. Campbell, Phys. Rev. B **65**, 155113 (2002).
[41] K. M. Tam, S. W. Tsai, and D. K. Campbell, Phys. Rev. Lett. **96**, 036408 (2006).
[42] N. R. Cooper and G. V. Shlyapnikov, Phys. Rev. Lett. **103**, 155302 (2009).
[43] A. J. Alexander, Phys. Chem. Chem. Phys. **7**, 3693 (2005).
[44] T. U. Ito, W. Higemoto, K. Ninomiya, and H. S. Suzuki, Phys. Rev. B **84**, 064411 (2011).
[45] J. M. Blatt and V. F. Weisskopf, *Theoretical Nuclear Physics* (Springer, New York, 1979).
[46] C. Bambi, Phys. Rev. D **83**, 103003 (2011).
[47] M. R. Flannery, D. Vrinceanu, and V. N. Ostrovsky, J. Phys. B **38**, S279 (2005).
[48] M. Saffman, T. G. Walker, and K. Mølmer, Rev. Mod. Phys. **82**, 2313 (2010).